SUPPORTING INFORMATION

Materials and Methods

Chemicals and Nanoparticles.

Propidium iodide (PI) and monobromobimane (MBB) were from Sigma (St. Louis, MO). 3,3'-dihexyloxabarbocyanine iodide ($DiOC_6$), Fluo-3, Rhod-2, dichlorofluorescein diacetate (DCF-DA), and hydroethidine (HE), MitoSOX red were obtained from Molecular Probes (Eugene, OR). Dulbecco's Modified Eggle's medium (DMEM), penicillin/streptmycin, and L-glutamine were purchased from Invitrogen (Carlsbad, CA). FBS was from Atlanta Biologicals, Inc (Lawrenceville, GA). Commercial grade ultrafine TiO_2 (Aeroxide P25) and carbon black (CB) (Printex 90) were obtained from Degussa (Hanau, Germany). Fullerol (hydroxylated C_{60}) ($C_{60}OH_{20-24}$) were purchased from MER Corporation (Tucson, AZ). Polystyrene (PS) nano- and microspheres (Bangs Laboratory, Fishers, IN) that exhibit different surface chemistries were used as model particles to compare the effects of size, charge and surface modification. These include 60 nm unmodified (PS), 60 nm carboxylated (COOH-PS), 60 nm amino (NH_2) modified (NH_2-PS) and 600 nm NH_2-modified (600-PS) particles. For all experiments and analyses, water was de-ionized and filtered with a 0.45 mm nominal pore size polycarbonate syringe filter (Millipore, Billerica, MA). All chemicals were reagent grade and used without further purification or modification.

Ambient particle collection and characterization

Ambient UFP (< 0.15 μm) were collected in the Los Angeles basin using the Versatile Aerosol Concentration Enrichment System (VACES) as described previously. [1] Ambient UFP collected in downtown Los Angeles are mostly derived from vehicular sources, are heterogeneous in size and are comprised of a solid core made of either inorganic material (sulfuric acid and transition metals)

or soot, surrounded by a layer of adsorbed or condensed semi-volatile organic constituents.[1,2] The concentration enrichment process does not alter the physical, chemical, and morphologic properties of the particles. The particle concentration in the aqueous medium was calculated by dividing the particle loading by the total volume collected over that time period. The sample was collected at the University of Southern California (USC), which represents a typical urban site. The aerosols at this site are mostly generated from fresh vehicular emissions. The content of 16 signature PAHs in each collection was determined by an HPLC-fluorescence method.[1] Heavy metal and other components were determined by Inductively Coupled Plasma Mass Spectroscopy (ICP-MS).

Assessment of ROS generation under abiotic conditions

ROS generation was assessed by the technique of Pickering et al.[3] Four borosilicate glass vials with PTFE-lined caps were filled with a solution consisting of 100 mM furfuryl alcohol (FFA) in an aerated phosphate buffer (pH = 7). NP were added to a final mass concentration of 0.5 mg/L. Three vials containing the respective nanoparticle solutions were exposed to UV light. The UV light source had an output spectrum ranging from 310-400 nm, a peak at 365 nm and a total irradiance of 24.1 W/m^2. A fourth vial served as a non-UV exposed control sample in which all other conditions were maintained similar to the test vials. To ensure that the samples were kept under the same conditions, especially temperature, the control was kept with the irradiated vials. Oxygen consumption was calculated as the difference in dissolved oxygen concentration of the control vial and the average of the three exposed vials.

CNT- NADH peroxidase (Npx)-bioelectrode

CNTs have shown great promise as biocompatible electrodes, capable of maintaining the functional properties of redox enzymes while linking biomolecules into nanoelectronic platforms.[4-7] This includes linking of glucose oxidase and NADH oxidase (Npx) to a CNT electrode array.[8] In these

systems, redox processes are detected as electronic signals that are registered by chronoamperometry and cyclic voltammetry. [8,9] For the purposes of this study, we made use of a CNT-Npx bioelectrode that is capable of H_2O_2 detection with a high level of sensitivity. The formation of the Npx-gold electrode assembly and immobilization on the CNT array electrode was reported previously.[9] Briefly, a three-electrode cell was used in the measurement: Npx-bioassembly CNT array as the working electrode, and an Ag/AgCl reference electrode with a platinum wire as the counter electrode. Electrochemical measurements were performed on an Epsilon system (BASi) at 22^{o}C. The bioelectrodes were equilibrated in the reaction buffer (acetate buffer, pH 6) or water, then scanned to obtain initial cyclic voltammograms (CV) of the enzyme assembly prior to sample measurements. Samples of TiO_2, fullerol, CB, and ultrafine particles were prepared by serially diluting with water to a final concentration of 50 pM and allowed to incubate 1 hr prior to measurements. Scans were taken at 1 hr (t=0) and at 1,3,7,12, and 21 days at a scan rate of 100 mV/sec. Between sample analyses, all samples were tightly sealed and stored in the dark at 4^{o}C. Prior to each measurement, the samples were slowly equilibrated to reach room temperature.

Physiocochemical characterization

All nanoparticles were characterized in terms of size, shape, charge, and relative hydrophobicity. Nanoparticle shape and structure was characterized using a transmission electron microscope (JEOL JEM 2010, JEOL USA, Inc., Peabody, MA). Microfilms for TEM imaging were made by placing a drop of the respective NP suspension onto a 200-mesh copper TEM grid (Electron Microscopy Sciences, Washington, PA) and then dried at room-temperature overnight. No fewer than five images of each sample were collected to ensure that those reported were representative of the sample at large.

Particle size distribution (PSD) measurements were carried out using a Malvern Zetasizer Nano ZS (Malvern Instruments, Worcestershire, UK). This instrument is equipped with a helium/neon laser (l = 633.4 nm) and measures the backscatter from a suspension at an angle of 173°. It is capable of measuring particles in the size range 0.6 nm-6 mm. Size measurements were performed on dilute NP suspensions in 10 mM NaCl solutions at pH 6. The Zetasizer was also used to measure the electrophoretic mobility of the NP suspended in solutions of 10 mM NaCl. Electrophoretic mobility may be used as an approximation of particle surface charge and can be used to calculate zeta potential. The isoelectric point (IEP) for each of the different NP was determined by measuring the change in electrophoretic mobility as a function of pH in a 10 mM NaCl solution. Solution pH was adjusted using either NaOH or HCl. The Helmholtz-Smoluchowski equation was used to correlate electrophoretic mobility to zeta potential. The PSD and electrophoretic mobility of all NP were also measured in the complete culture media for comparison.

The relative hydrophobicity of the various NP was assessed using a hydrocarbon partitioning test with laboratory-grade n-dodecane (Fisher Scientific, Pittsburgh, PA). Samples were prepared by adding 4 mL of NP suspension at a concentration of approximately 5 mg/L to a test tube containing 1mL of dodecane. The test tube was vortexed (S/P Vortex Mixer, American Scientific Products) for 2 min, followed by a 15-min rest period to allow for phase separation. The relative hydrophobicity was assessed as the fraction of the initial NP concentration that partitioned into the dodecane from the aqueous phase.

Cell culture and co-incubation with NP

RAW 264.7 cells were cultured in a 5% CO_2 in Dulbecco's Modified Eagle Medium (DMEM) containing 10% FCS, 5000 U/ml penicillin, 500 μg/ml streptomycin, and 2 mM L-glutamine (complete medium). For exposure to NP, aliquots of 3×10^5 cells were cultured in 24-well plates in

0.5 ml of medium at 37 °C for the indicated time periods. All the NP solutions were prepared fresh from stock solutions (10 mg/ml) and the solutions were sonicated for 10 sec before addition to cell cultures.

Cellular staining with fluorescent probes and flow cytometry

Cells were stained with the fluorescent dyes diluted in DMEM. The following dye combinations were added for 15-30 min at 37 °C in the dark: (i) 47.5 μg/ml PI in 200 μl DMEM (assessment of cell death); (ii) 20 nM $DiOC_6$ (assessment of $\Delta\Psi m$); (iii) 2 μM MitoSOX red (superoxide generation) or 2 μM HE (superoxide production); (iv) 2.5 μM DCF (mostly assesses H_2O_2 production); (v) 5 μM Fluo-3 (assess cytoplasmic free calcium); (vi) 4 μM Rhod-2 (mitochondrial free calcium); (vii) 40 μM MBB (assess intracellular thiol levels). Flow cytometry was performed using a FACScan (Becton Dickinson, Mountain View, CA) equipped with a single 488 nm argon laser. $DiOC_6$ and Fluo-3 fluorescence were analyzed in the FL-1 channel, while PI, Rhod-2 and MitoSOX red fluorescence were analyzed in FL-2. HE fluorescence was analyzed using FL-3 channels. MBB fluorescence was excited by the UV laser tuned to 325 nm, and emission was measured at 510 nm (FL-4 channel) in the LSR flow cytometer. Forward and side scatter were used to gate out cellular fragments.[10,11]

Measurement of TNF-α production

Triplicate aliquots of RAW 264.7 cells were exposed to NP for 6 hr. The culture media were collected, centrifuged to remove all debris, and sent frozen to the Cytokine Core Laboratories at the University of Maryland (Baltimore, MD, USA) for measuring TNF-α by ELISA.

Western blotting analysis

After NP stimulation, RAW cells were collected and washed with PBS. The cell pellets were resuspended in cell lysis buffer containing Triton X-100 and protease inhibitors and the lysates were briefly sonicated. The Bradford method was used to determine the protein content in the supernatant of these lysates. 100 μg of total protein was separated by 10% SDS-PAGE and transferred to a PVDF membrane. After blocking, the membranes were incubated with primary antibodies against HO-1, phospho-JNK or JNK. The membranes were overlayed with secondary Ab before the addition of the HRP-conjugated avidin-biotin complex. The proteins were detected using ECL reagent according to the manufacturer's instructions. Protein abundance was quantified by densitometric scanning using a laser Personal Densitometer SI and Image Quant software (Amersham Biosciences).

Transmission Electron Microscopy

Electron microscopy was performed as previously described by us.[12] Thin sections were cut with a Reichert-Jung ultracut and ultramicrotome (Leica, Stuttgart, Germany). Copper grids were stained with lead citrate and uranyl acetate and photographed in a Hitachi electron microscope (Hitachi Instrument Inc., Tokyo, Japan). The TEM of NP was performed after drying up particle solutions on 400 mesh grids, then analyzed by a JEOL 100CX transmission electron microscope.

Statistical analyses

All data are expressed as the mean ± SD. An unpaired Student's t test was used to assess the difference between two groups. One-way ANOVA was performed when more than two groups were compared with a single control. Differences between individual groups within the set were assessed by a multiple comparison test (Tukey) when the F statistic was < 0.05. A $p< 0.05$ was considered significant.

Supplementary Figure Legends

Fig. S1. (A) Size distribution of ambient UFP measured during aerosolized collection as well as suspended in H_2O and complete (DMEM with 10% FCS) culture medium. Size distribution was measured using Dynamic Light Scattering (DLS) at a scattering angle of 90°. Additional measurements were also carried out using a Malvern Zetasizer, which measures the backscatter from a suspension at an angle of 173°. (B) Pie chart of the chemical composition of UFP with tables showing the content of transition metals and polycyclic aromatic hydrocarbons (PAHs). We have previously shown that there is an almost linear relationship between the PAH content of UFP, their redox-cycling capacity (measured by the DTT assay) and ability to induce HO-1 expression in RAW 264.7 cells.[1]

Fig. S2. (A, B) Size distribution of CB, TiO_2 and fullerol in H_2O and complete culture medium was performed as described in S1.

Fig. S3. (A, B) Size distribution of polystyrene particles in H_2O and complete culture medium was performed as described in S1.

Fig. S4. (A) Model of the bioassembly containing the redox enzyme, NADH peroxidase (Npx) (depicted in grey ribbon), multi-histidine peptide (MHP) (in green ribbon) with metals (small yellow spheres) coordinated by histidine side chains (in gray ball-and-stick). A mono-functionalized gold nanoparticle (large gold sphere) terminates the assembly. (B) Attachment of the Npx-bioassembly to CNT electrode arrays. The reaction between the N terminals (NT) of the MHP peptide to the carboxyl groups at the tips of CNT is catalyzed by a modified method of the conventional EDC/NHS reaction. As the majority of carboxyl groups are found at the tips of the CNT electrodes generated via acid-etching following templated growth, the bioassembly is specifically linked to the electrode platform tips, maximizing exposure of the bioassembly to

solution for analysis. (C) Scanning electron microscopy (SEM) images of the Npx-bioassembly linked to the CNT electrode array. The gold nanoparticles have a high backscatter coefficient so they appear bright in the SEM (light colored balls in the images). As these images confirm, the bioassembly is specifically linked to the tips of the CNT arrays and the reaction conditions can be manipulated to modify the amount of assembly placed. The CNTs are 50 nm in diameter, have walls of 3 nm thickness, and exhibit an exposed length of 60 nm, a total length of 10 m, and a center-to-center spacing of 100 nm between adjacent tubes.

Fig. S5. Mitochondrial superoxide production in RAW 264.7 cells after treatment with nanoparticles. At the indicated time point, MitoSOX Red-stained cells were treated with NH_2-PS and UFP particles in the presence or absence of 10 mM NAC. The flow data were expressed as a bar graph to show the percentage of MitoSOX Red bright-positive cells. Data are representative of 3 separate experiments. *$p<0.01$, compared to control.

Fig. S6. (A) Dose dependent HO-1 expression in RAW 264.7 cells exposed to UFP. (B) Dose dependent TNF- production in RAW 264.7 cells exposed to UFP. (C) (C) TNF-α cytokine production in RAW 264.7 cells after exposure to LPS (200ng/ml) or UFP for 6 hr, in the absence or presence of treatment of 200 U/ml Polymxin B (PMB). This experiment was undertaken to distinguish the particle effect from endotoxin (LPS) mediated cellular stimulation.

Fig. S7. Fold increase in Fluo-3 mean fluorescence after 16 hr treatment with UFP, fullerol, CB, TiO_2 and PS nanoparticles. Data are representative of 2 experiments. *$p<0.01$, compared to control.

Table S1. Characteristics of manufactured NP

	CB	TiO_2
BET	300 m^2/g	50 m^2/g
Primary particle size	14 nm	20-30 nm
PAHs (μg/g)		
Phenanthrene	0.039	ND
Anthracene	0.001	ND
Fluoranthene	0.010	ND
Pyrene	0.065	ND
Benzo(ghi)perylene	0.008	ND
Benzo(a)pyrene	ND	ND

PAH contents (16 PAHs) were determined by HPLC-FLD after Soxhlet extraction.[13] PAH levels are in μg/g. 12 other PAH, including benzo(ghi)perylene that were also measured for UFP (Fig. S1B) were undetectable in CB.

Carbon black NP: Printex 90 from Degussa, (Hanau, Germany). TiO_2 NP: P25 from Degussa (Hanau, Germany); anatase/rutile composition= 4:1.[14]

ND, not determined

Table S2. Endotoxin content (U/ml)

UFP	20
CB	<0.1
TiO_2	<0.1
Fullerol	<0.1
PS	<0.1
NH_2-PS 60 nm	<0.1
NH_2-PS 600nm	<0.1
COOH-PS	<0.1

The endotoxin analysis was carried out using Cambrex Limulus Amebocyte Lysate (LAL) kit QCL-1000. Endotoxin standards and 10 μg/ml of each NP suspension were tested according to the manufacturer's instructions. Absorbance of each reaction was read at 405 nm in an ELISA reader and endotoxin concentration was calculated according the standard curve.

References

(1) Li, N.; Sioutas, C.; Cho, A.; Schmitz, D.; Misra, C.; Sempf, J.; Wang, M.; Oberley, T.; Froines, J.; Nel, A. Environ. Health. Perspect. 2003, 111, 455-460.

(2) Geller, M.D.; Kim, S.; Misra, C.; Sioutas, C.; Olson, B.A.; Marple, V.A. Aerosol Science & Technology 2002, 36, 748-762.

(3) Pickering, K.; Wiesner, M. Environ. Sci. Technol. 2005, 39, 1359-1365.

(4) Sotiropoulou, S.; Chaniotakis, N.A. Anal. Bioanal. Chem. 2003, 375, 103-105.

(5) Gooding, J.J.; Wibowo, R.; Liu,J.; Yang,W.; Losic, D.; Orbons, S.; Mearns, F.J.; Shapter, J.G.; Hibbert, D.B. J Am Chem. Soc. 2003, 125, 9006-9007.

(6) Cai, C.; Chen, J. Anal. Biochem. 2004, 332, 75-83.

(7) Guiseppi-Elie, A.; Lei, C.; Baughman, R.H. Nanotechnology 2002, 13, 559-564.

(8) Withey, G.D.; Lazareck, A.D.; Tzolov, M.B.; Yin, A.; Aich, P.; Yeh, J.I.; Xu, J.M. Biosens. Bioelectron. 2006, 21, 1560-1565.

(9) Yeh, J.I.; Zimmt, M.B.; Zimmerman, A.L. Biosens. Bioelectron. 2005, 21, 973-978.

(10) Hiura, T.S.; Li, N.; Kaplan, R.; Horwitz, M.; Seagrave, J.C.; Nel, A.E. J. Immunol. 2000, 165, 2703-2711.

(11) Li, N.; Venkatesan, M.I.; Miguel, A.; Kaplan, R.; Gujuluva, C.; Alam, J.; Nel, A. J. Immunol. 2000, 165, 3393-3401.

(12) Yang, A.H.; Gould-Kostka, J.; Oberley, T.D. In Vitro Cell Dev. Biol 1987, 23, 34-46.

(13) Borm, P.J.; Cakmak, G.; Jermann, E.; Weishaupt, C.; Kempers, P.; van Schooten, F.J.; Oberdorster, G.; Schins, R.P. Toxicol. Appl. Pharmacol. 2005, 205, 157-167.

(14) Hohr, D.; Steinfartz, Y.; Schins, R.P.; Knaapen, A.M.; Martra, G.; Fubini, B.; Borm, P.J. Int. J Hyg. Environ. Health 2002, 205, 239-244.

Fig. S1

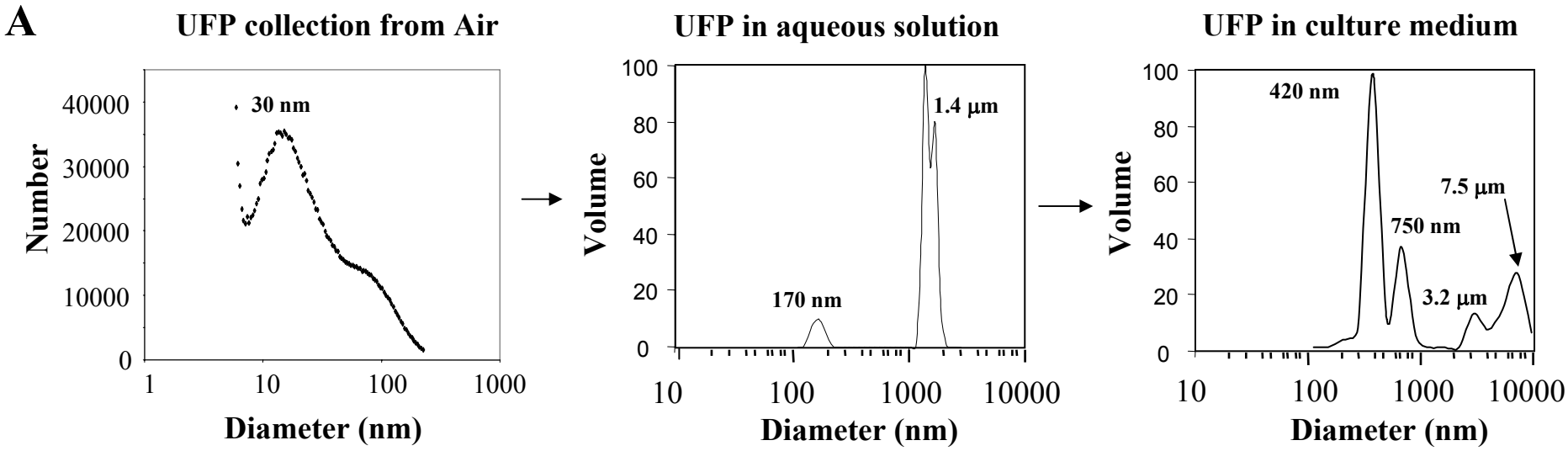
A
UFP collection from Air
UFP in aqueous solution
UFP in culture medium
Number
Volume
Volume
Diameter (nm)
Diameter (nm)
Diameter (nm)
30 nm
170 nm
1.4 μm
420 nm
750 nm
3.2 μm
7.5 μm
0
10000
20000
30000
40000
0
20
40
60
80
100
1
10
100
1000
10000

B

Metals	µg/g
Na	4796
Al	11595
Si	31334
S	12164
Cl	5292
K	2994
Ca	11600
Ti	139
Fe	8386
Cu	1256
Zn	1564
Br	1485

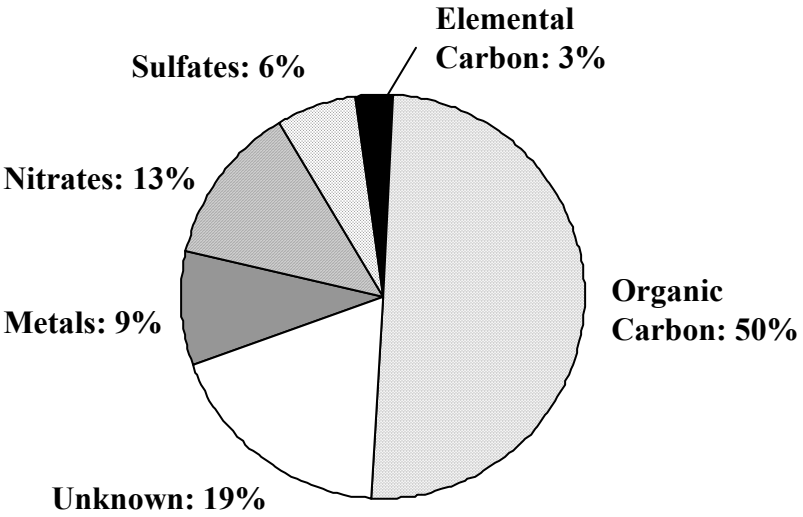

PAH	µg/g
NAP	<LOD
ACE	<LOD
FLU	<LOD
PHE	10.5268
ANT	<LOD
FLT	3.2567
PYR	7.6688
BAA	0.3878
CRY	0.8040
BBF	0.2676
BKF	0.1784
BAP	0.1608
DBA	<LOD
BGP	1.0540
IND	<LOD

Abbreviations: BAA, benzo(a)anthracene; BAP, benzo(a)pyrene; BBF, benzo(b)fluoranthene; BGP, benzo(ghi)perylene; BKF, benzo(k)fluoranthene; CRY, chrysene; FLT, fluoranthene; IND, indeno(1,2,3-cd) pyrene; PHE, phenanthrene; PYR, pyrene.
LOD, limit of detection

Fig. S2

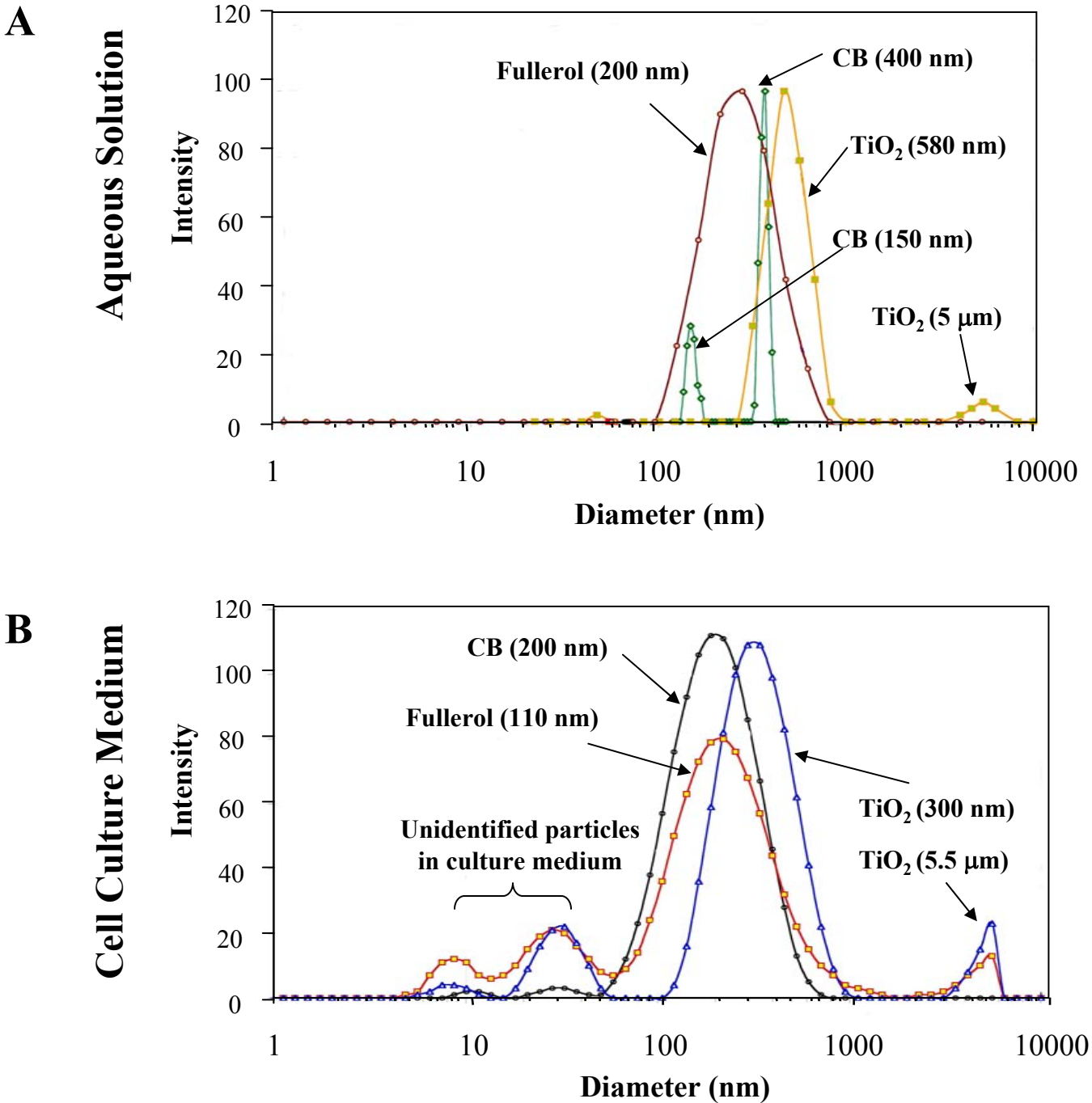
A
Aqueous Solution
Intensity
120
100
80
60
40
20
0
Fullerol (200 nm)
CB (400 nm)
TiO2 (580 nm)
CB (150 nm)
TiO2 (5 μm)
1
10
100
1000
10000
Diameter (nm)
B
Cell Culture Medium
Intensity
120
100
80
60
40
20
0
CB (200 nm)
Fullerol (110 nm)
Unidentified particles
in culture medium
TiO2 (300 nm)
TiO2 (5.5 μm)
1
10
100
1000
10000
Diameter (nm)

Fig. S3

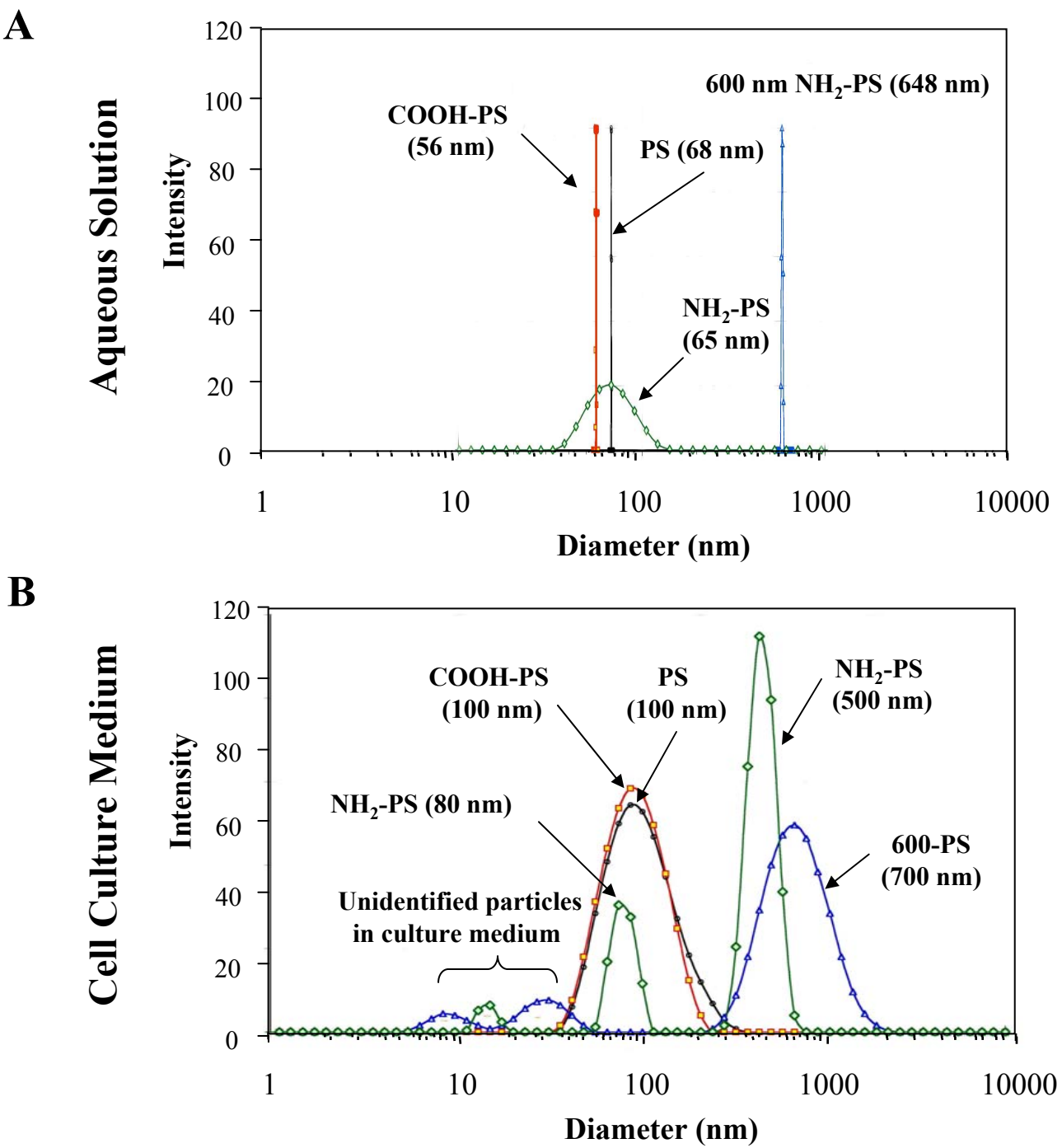
A
Aqueous Solution
Intensity
120
100
80
60
40
20
0
COOH-PS
(56 nm)
PS (68 nm)
600 nm NH2-PS (648 nm)
NH2-PS
(65 nm)
1
10
100
1000
10000
Diameter (nm)
B
Cell Culture Medium
Intensity
120
100
80
60
40
20
0
COOH-PS
(100 nm)
PS
(100 nm)
NH2-PS
(500 nm)
NH2-PS (80 nm)
600-PS
(700 nm)
Unidentified particles
in culture medium
1
10
100
1000
10000
Diameter (nm)

Fig. S4

A

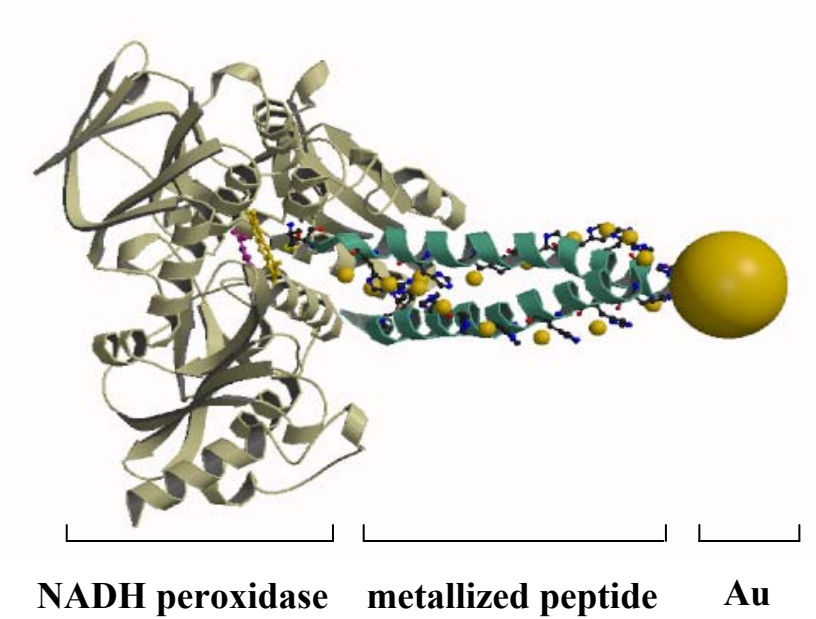

B CNT-pep2Co-Npx formation through wsc-sulfo-NHS

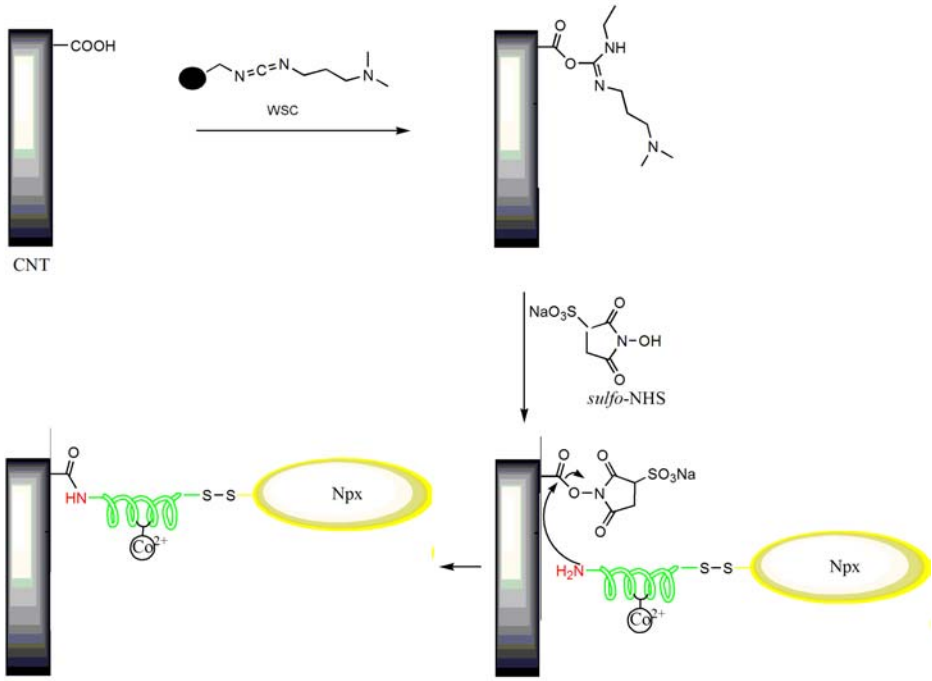

C TEM of CNT-Npx Assembly

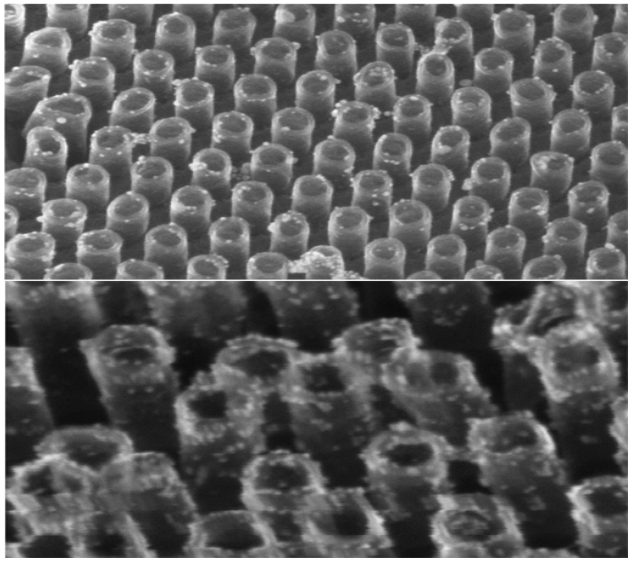

Fig. S5

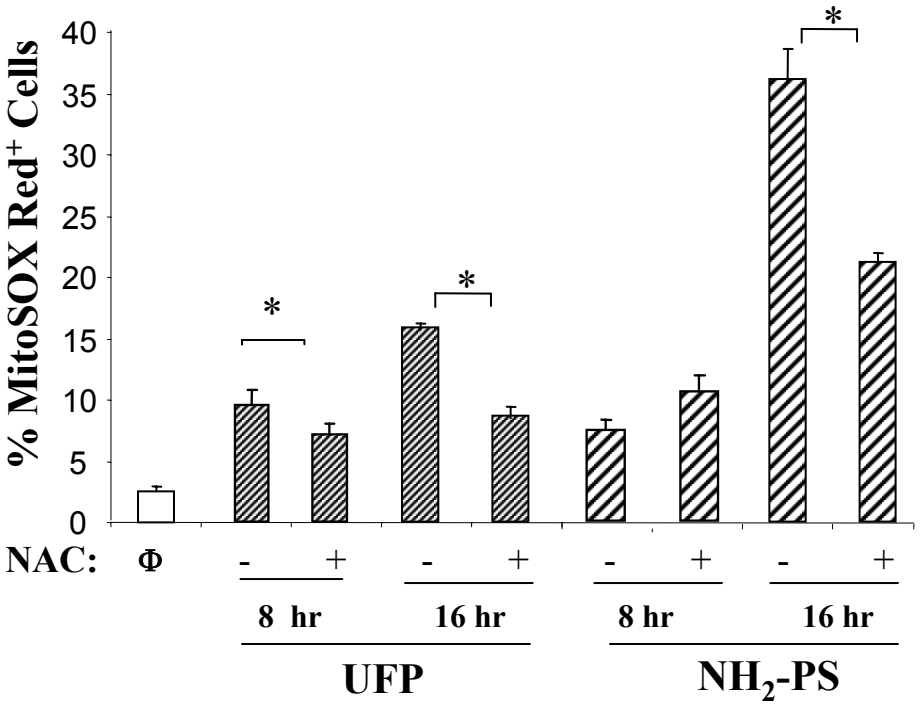
% MitoSOX Red+ Cells
40
35
30
25
20
15
10
5
0
*
*
*
NAC:
Φ
-
+
-
+
-
+
-
+
8 hr
16 hr
8 hr
16 hr
UFP
NH2-PS

Fig. S6

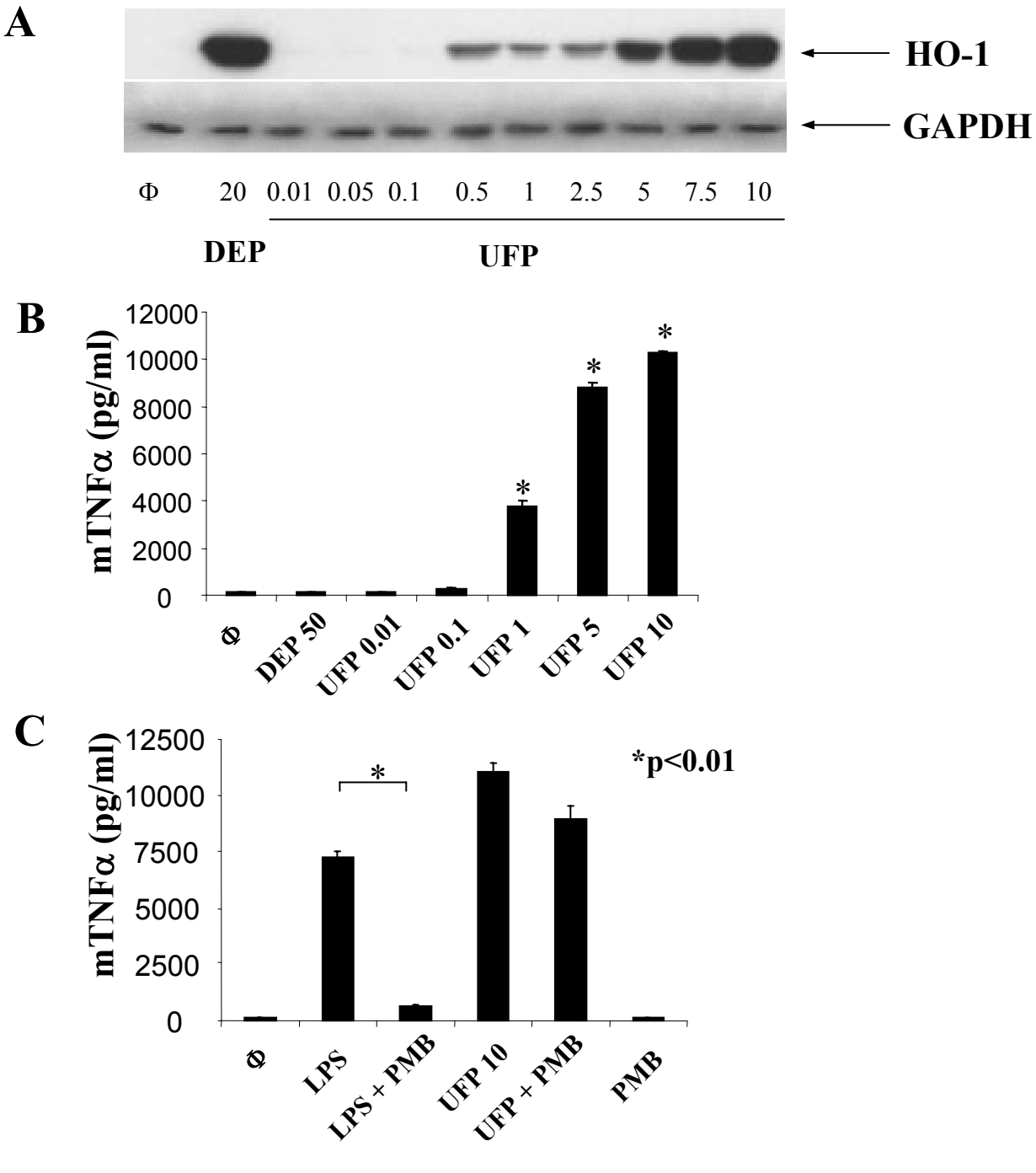
A
HO-1
GAPDH
Φ 20 0.01 0.05 0.1 0.5 1 2.5 5 7.5 10
DEP
UFP
B
mTNFα (pg/ml)
12000
10000
8000
6000
4000
2000
0
Φ
DEP 50
UFP 0.01
UFP 0.1
UFP 1
UFP 5
UFP 10
C
mTNFα (pg/ml)
12500
10000
7500
5000
2500
0
*p<0.01
Φ
LPS
LPS + PMB
UFP 10
UFP + PMB
PMB

Fig. S7

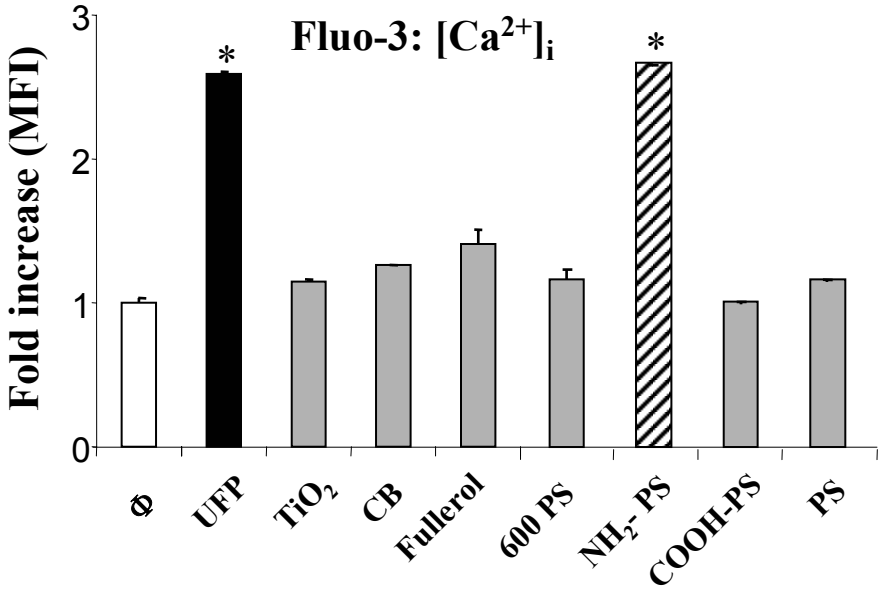
Fluo-3: [Ca2+]i
Fold increase (MFI)
3
2
1
0
*
*
Φ
UFP
TiO2
CB
Fullerol
600 PS
NH2- PS
COOH-PS
PS